Biochemical and Biophysical Research Communications **264,** 151–156 (1999)
Article ID bbrc.1999.1479, available online at http://www.idealibrary.com on IDEAL®

Molecular Cloning of a Novel *Xenopus spalt* Gene (*Xsal-3*)

Yasuko Onuma,* Ryuichi Nishinakamura,† Shuji Takahashi,‡
Takashi Yokota,† and Makoto Asashima*,‡,[1]
*Department of Life Sciences, ‡CREST Project, University of Tokyo, Komaba, Meguro-ku, Tokyo 153-8902, Japan; and
†Department of Stem Cell Regulation, Institute of Medical Science, University of Tokyo,
Shiroganedai, Minato-ku, Tokyo 108-0071, Japan

Received September 6, 1999

The *sal* (*spalt*) gene family is characterized by unique double zinc finger motifs and is conserved among various species from *Drosophila* to humans. Here we report a new *Xenopus* member of this family, *Xsal-3*. It is 38% homologous at the amino acid level to the previously reported *Xenopus* homologue of the *spalt* gene, *Xsal-1*. Alternatively spliced *Xsal-3* transcripts give rise to RNAs coding either two or three double zinc fingers, and the longer form is expressed maternally. *Xsal-3* is expressed in the neural tube, the mandibular, hyoid, and branchial arch, and the pronephric duct, which is different from the expression pattern of *Xsal-1*. These findings suggest that *Xsal-3* may have distinct roles in early *Xenopus* development.

The *Drosophila spalt* (*sal*) gene is a region-specific homeotic gene, which acts in two separate domains, an anterior domain and a posterior domain (1). Molecular cloning of the *spalt* gene (2) has shown that it encodes a protein of 1355 amino acids. The gene product is characterized by seven zinc finger motifs of the CC/HH type (3), and the arrangement of the zinc fingers is quite unusual: six of the seven fingers are grouped into three widely separated pairs. Sequence comparison of these zinc finger pairs (double zinc finger motif) showed conservation of two boxes in all three pairs. The first conserved box is the spacer motif for closely linked zinc fingers, the H/C-link motif (4), while the second box is an eight amino acid motif (FTTKGNLK) found in the second fingers of all pairs, the so-called SAL-box. In addition to its function as a homeotic gene during the early blastoderm stage, the *Drosophila spalt* gene is also expressed in restricted areas later in development, for example the central nervous system (CNS), the tracheal system, and the visceral mesoderm of the midgut (2).

Vertebrate homologues of *spalt* have been isolated and characterized in humans (*Hsal-1* and *Hsal-2*), mouse (*msal*), *Xenopus* (*Xsal-1*) and medaka fish (medaka *sal*). In humans, Mutation of *Hsal-1* is known to cause Townes-Brocks syndrome (TBS) (5), and in medaka, medaka sal has been found to be regulated by *Sonic hedgehog* (*Shh*) (6).

In *Xenopus*, a homologue of the *Drosophila spalt* gene (*Xsal-1*) has been isolated (7). The *Xsal-1* gene encodes a protein that contains double zinc finger motifs, and its expression is restricted to the CNS and the facial ganglion mainly in early development. Here we report the cloning and expression analysis of the novel *Xenopus spalt* gene (*Xsal-3*). *Xsal-3* protein has 38% homology with *Xsal-1*, and also contains the double zinc finger motifs. *Xsal-3* expression is shown in the CNS, the mandibular, hyoid and branchial arch, and the pronephric duct in early development.

MATERIALS AND METHODS

Xenopus embryos. *Xenopus laevis* eggs were obtained by injecting adult females with 600 IU of human chorionic gonadotropin (Gestron, Denka-seiyaku, Japan). Fertilized eggs were dejellied with 4% cysteine hydrochloride in the Steinberg's solution (pH 7.8), washed with sterilized Steinberg's solution (pH 7.4), and cultured at 20°C. The embryos were staged according to Nieuwkoop and Farber (8).

Differential display. Animal caps cut at stage 9 were exposed to 10 ng/ml activin A plus 10^{-4} M retinoic acid for 3 h. After the treatment, all explants were washed in Steinberg's solution and cultured for 6–9 h. Total RNA was extracted from animal caps treated with activin A plus retinoic acid and from untreated animal caps and was used for differential display. The three differentially expressed bands were cut from the gel, and the DNA was eluted and reamplified.

---

[1] To whom correspondence should be addressed at Department of Life Sciences, University of Tokyo, Komaba, Meguro-ku, Tokyo 153-8902, Japan. Fax: +81-3-5454-4330. E-mail: cmasa@komaba.ecc.u-tokyo.ac.jp.

0006-291X/99 $30.00

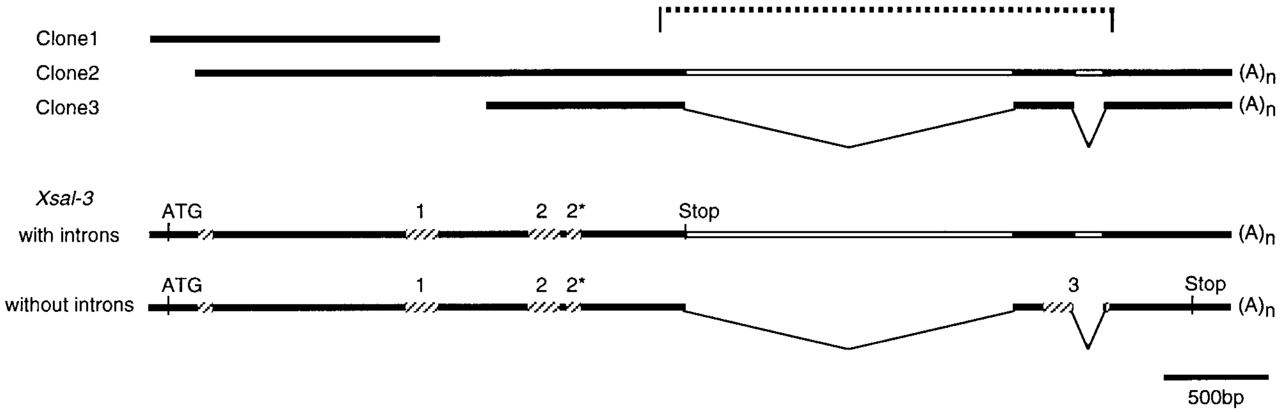

FIG. 1. Molecular structure of *Xsal-3*. Location of the cDNA clones isolated (Clones 1, 2, and 3), and the molecular structure of the predicted complete *Xsal-3*. The intronic sequences in Clone 2 are shown by in the open boxes, and their absence in Clone 3 is indicated by the V-shaped lines. The translation start site (ATG), the end of open reading frame (Stop), and the poly A tail [$(A)_n$] are indicated in the diagrams of two synthesized *Xsal-3* sequence (with and without introns). The hatched boxes show the positions of the zinc finger domains. The unnumbered boxes represent the CC/HC finger domain, while the boxes numbered 1–3 are the three double zinc fingers, and the 2* box is the CC/HH finger domain adjacent to the second double finger. The region amplified by PCR with *Xsal-3* specific primers is indicated by the broken line.

Isolation of Xsal-3 cDNAs. A fragment obtained by differential display was used as a probe. Two clones were obtained from a cDNA phage library (head region of stage 28–30 embryos) (9), and one clone was obtained from a *Xenopus* unfertilized egg cDNA plasmid library by plaque or colony hybridization. The three clones were sequenced with a DNA sequencer Model 373A by using Dye Deoxy Terminator Cycle Sequencing Kits (Applied Biosystems). Nucleotide sequences were analyzed by the Gene Works 2.5.1 program (Intelligenetics Inc.).

Expression of Xsal-3 RNA during development, and RT-PCR analyses. Total RNA was isolated from various developmental stages by ISOGEN (NIPPON GENE), and 2 μg of total RNA was used as a template to generate first strand cDNA according to the manufacturer's instructions (GIBCO, BRL); one tenth of this cDNA was used as a template in subsequent RT-PCR analyses. The primers used here and the product sizes were *Xsal-3* (forward, 5′-GATGAGCATTCTCAGAATGGC-3′; reverse, 5′-CTGCAAGTGCCTTACAGATCC-3′; 22 cycles) 2165, 2022, and 456 bp; *Xsal-1* (forward, 5′-TCCCACAGTTCCATCCCAAA-3′; reverse, 5′-AGTGTGCAGCAAAACCCTGC-3′; 22 cycles) 68 bp; and ornithine decarboxylase (ODC) (forward 5′-GTCAATGATGGAGTGTATGGATC-3′; reverse 5′-TCCATTCCGCTCTCCTGAGCAC-3′; 20 cycles) 386 bp. The resulting product was analyzed by Southern blot and sequencing to confirm its identity. Relative levels of transcripts encoding *ornithine decarboxylase* (*ODC*) were assayed by RT-PCR as described (10, 11).

In situ hybridization and histological examination. Whole-mount *in situ* hybridization was performed according to Harland (12). Digoxigenin (DIG)-labeled antisense RNA corresponding to the 4953-bp Clone 2 of *Xsal-3* was synthesized *in vitro*. The probe was hybridized to whole albino *Xenopus* embryos. For histological examination, embryos were directly or refixed with Bouin's solution and embedded in paraffin and sectioned at 10 μm.

RESULTS AND DISCUSSION

Animal caps treated with 10 ng/ml activin A plus 10^{-4} M retinoic acid differentiate into pronephros (12). To obtain the genes involved in pronephros formation, differential display using this system was performed. One partial cDNA clone from differential display was sequenced, and the clone was homologous to the *Xenopus* homologue of the *spalt* gene, *Xsal-1*. The semi-quantitative RT-PCR showed that the obtained clone expression is up-regulated in animal caps treated with 10 ng/ml activin A plus 10^{-4} M retinoic acid, but isn't induced in untreated animal caps, on the same condition as differential display (data not shown).

This clone was used as a probe to isolate two clones from a cDNA phage library (head region of stage 28-30 embryos) (Clone 1 and Clone 2) and from an unfertilized egg cDNA plasmid library one clone (Clone 3). Diagrams of these three clones are shown in Fig. 1. None of these clones contained the complete open reading frame (ORF). The homology between Clone 1 and Clone 2 in the overlapping region was 100% (nucleotide level), whereas the homology between Clone 2 and Clone 3 was 98.9% (nucleotide level). Therefore, Clone 1 and Clone 2 may be derived from the same gene, and Clone 3 may come from a closely related gene. We named the gene that yielded Clone 1 and Clone 2 *Xsal-3* (DDBJ Accession No. AB030827), and the gene that yielded Clone 3 *Xsal*-3′ (DDBJ Accession No. AB030828). Clone 2 and Clone 3 also contained the complete 3′ untranslated region including a polyadenylation stretch, but lacked the starting codon at the 5′ end of ORF. Sequence comparison with the known vertebrate *spalt* genes, however, indicated that Clone 1 may contain a starting codon. The presumptive sequence of *Xsal-3* was synthesized from Clone 1 and Clone 2, and the total Length of *Xsal-3* was 5174 bp. Conceptual translation of the 2478 bp ORF yielded an 826 amino acid sequence that contains one zinc finger of the CC/HC-motif, a single zinc finger of the CC/HH-

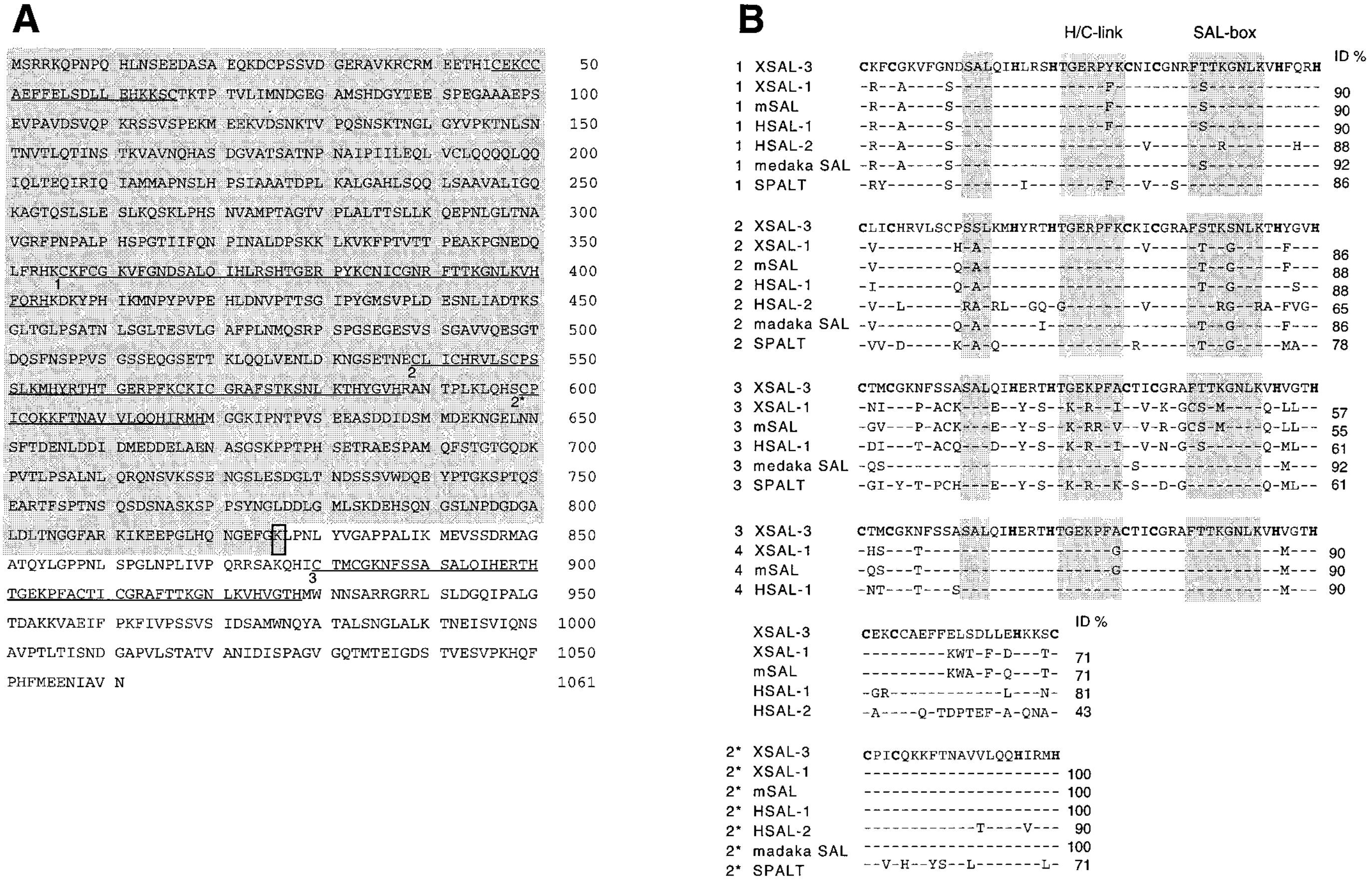

FIG. 2. (A) Amino acid sequences of the long form of XSAL-3. The length of the sequence is 1061 aa (long form of XSAL-3). The short form of XSAL-3 is shown in the shaded area, and is shorter than the long form, 826 aa, because the stop codon is present in the first intron. The only one residue in the long form sequence different from the short form, "K," is marked by an open box, and is replaced by residue, "R" in the short form. The zinc finger motifs are underlined, the double zinc fingers are numbered 1-3. The CC/HH finger domain adjacent to the second double finger is marked 2*. (B) Sequence comparison of homologous zinc finger motifs of *Xsal-3* (long form), *Xsal-1,* mouse *sal* (*msal*), human *sal-1* (*Hsal-1*), human *sal-2* (*Hsal-2*), medaka *sal,* and *Drosophila spalt.* zinc complexing cysteine (C) and histidine (H) residues are shown in bold print. Identical amino acid residues are shown as dashes, and the conserved tripeptide "SAL," the H/C-link, and the SAL-box are shaded. Sequence identity values correspond to the XSAL-3 fingers respectively. The single N-terminal CC/HC motif is not numbered. The double zinc finger motifs are numbered from the N- terminal, and the single CC/HH finger motif adjacent to the second double finger is marked 2*.

motif, and two double zinc finger motifs, as shown in Fig. 2A. This sequence also contains 90 bp of the 5′-untranslated region and 2606 bp of the 3′-untranslated region. When compared with the sequence of Clone 3, Clone 2 was found to have two inserted sequences (Fig. 1). The insertions were presumed to be introns, since *Xsal-1,* which is the gene most similar to *Xsal-3,* includes multiple alternatively spliced variants (7). If the two introns of *Xsal-3* are deleted by alternative splicing, the sequence would be 3465 bp long, and would code 1061 amino acids. The spliced form is longer than the unspliced form in amino acid level, and has an additional double zinc finger motif (Figs. 1 and 2A). The presumptive protein from the transcript of *Xsal-3* with introns is referred to as the "short form," and the presumptive protein encoded by the transcript of *Xsal-3* without introns is referred to as the "long form."

The deduced amino acid sequence of *Xsal-3* shows high overall similarity to the known vertebrate *sal* genes (38% in comparison to *Xenopus Xsal*-1, 35% in comparison to human *Hsal-1,* 27% in comparison to human *Hsal-2,* 33% in comparison to medaka *sal,* and 33% in comparison to mouse *msal*). *Xsal-3* encodes a protein that contains the three diagnostic double zinc finger domains and a single zinc finger of the CC/HH-motif located adjacent to the second pair of zinc fingers, which are characteristic of all SAL homologues. The entire domain containing the zinc fingers of SAL is highly conserved between vertebrates and *Drosophila* and shows the typical H/C-link of SPALT zinc fingers as well as the diagnostic SAL-box (2) in each second finger of the three double zinc finger regions (Fig. 2B). The high degree of conservation in the zinc fingers suggests that all *sal* homologues may recognize a con-

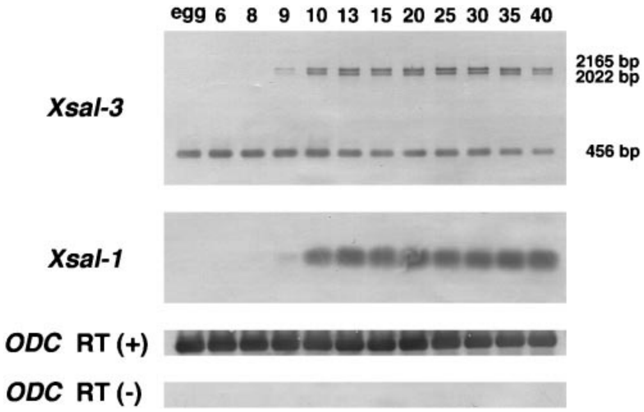

FIG. 3. Expression of *Xsal-3* and *Xsal-1* during development as detected by RT-PCR. RNA was extracted from embryos at the stages indicated. With the *Xsal-3* specific primer pair that flanks both introns, the lengths of the amplification products were 2165, 2022, and 456 bp. RT-PCR with *ornithine decarboxylase* (*ODC*) specific primers was carried out in parallel to control the amount of input RNA [RT(+)]. RT(−), RT-PCR without reverse transcriptase. Stages are shown over each lane. egg, unfertilized egg.

served binding site. The amino terminus of XSAL-3 contains an additional single zinc finger of the CC/HC-type characteristic of vertebrate SAL proteins. The *Xsal-3* gene gives rise to RNA coding two or three double zinc fingers. Sequence comparison between XSAL-3 and XSAL-1 showed that the third double zinc finger motif of XSAL-3 is highly homologous to the fourth motif of XSAL-1 (Fig. 2B). Thus, it is possible that a true third double zinc finger motif of XSAL-3 exists but has not yet been identified. In summary, these features identify Xsal-3 as a homologue of the *Drosophila* and the known vertebrate *spalt* genes (2, 6, 7, 13, 14).

To examine expression of *Xsal-3,* RT-PCR was carried out using RNA from various developmental stages (Fig. 3). *Xsal-3* specific primers were designed to discriminate alternative spliced variants. The transcripts corresponding to the 2165 and 2022 bp products have both introns and only the first intron, respectively, and encode the short form XSAL-3. The transcript corresponding to the 456 bp product has no intron and encodes long form XSAL-3. The transcripts of long form XSAL-3 were detected from the unfertilized egg to tadpole stage (stage 40), and gradually decreased after the early neurula stage (stage 15). In contrast, the two transcripts encoding the short form XSAL-3 were absent maternally, appeared at stage 10, and were detected through the tadpole stage, which was similar to expression patterns of previously reported *Xsal-1* (7). These findings suggest that there are at least three alternative spliced variants of Xsal-3, and that they have different temporal patterns of expression. These variants may have different roles in development.

The spatial expression pattern of *Xsal-3* was examined by whole-mount *in situ* hybridization and in sections of stained embryos. The total signals of all three kinds of transcripts (described above) could be detected by using Clone 2 as the probe. The signals were localized to the animal hemisphere of unfertilized eggs (Fig. 4A). From the onset of gastrulation to the late gastrula (Figs. 4B and 4C), expression was localized to the animal hemisphere with a dorsal bias. In the sagittal section of stage 11 embryos (Fig. 4D), the signals were observed only in ectoderm. From the neurula stages onwards, *Xsal-3* is expressed in the neural plate and tube along the anteroposterior axis of the developing central nervous system (CNS) and the neural crest (Fig. 4E). The transverse section of an early neurula embryo (stage 16) showed that *Xsal-3* expression was restricted to the neural plate (Fig. 4F, black arrow) and the neural crest (Fig. 4F, red arrows). After the tailbud stage, mainly expression was in the CNS and the mandibular, hyoid, and branchial arch. Weak signal appeared in the otic vesicle and the tail bud (Figs. 4G and 4H). In the transverse section of a stage 30 embryo (Fig. 4I), signals appeared at the floor and lateral plate of the neural tube and in the pronephric duct. In the horizontal section of a stage 30 embryo (Fig. 4J), the strong signals were shown in the neuroectoderm cells derived from the neural crest at the exclusion of the mesoderm and endoderm. In conclusion the main expression regions of *Xsal-3* is in the CNS, the mandibular, hyoid, and branchial arch and the pronephric duct. This expression pattern is similar to that of previously reported *Xsal-1,* which is expressed in the CNS, the facial ganglion, the pronephros (tubules and duct), the heart anlage and the tail bud. The differences between the temporal and spatial expression pattern of the two genes were as follows. (1) Long form of *Xsal-3* was expressed maternally, whereas *Xsal-1* was expressed only zygotically. (2) *Xsal-3* is expressed in the neuroectoderm of the mandibular, hyoid, and branchial arch strongly, whereas *Xsal-1* is not. (3) *Xsal-3* is not expressed in the heart anlage, but *Xsal-1* is expressed. (4) In the neural tube, *Xsal-3* is expressed in inner region (proliferating cells) of the neural tube, *Xsal-1* is in outer region (motor neurons and interneurons) of the neural tube (7). Therefore, *Xsal-3* and *Xsal-1* may have different roles during *Xenopus* embryogenesis.

Little is known about roles of vertebrate *spalt.* Mutations in the human homologue of *spalt* (*Hsal-1*) cause Townes-Brocks syndrome (TBS) (5). TBS is a rare autosomal-dominant malformation syndrome with a combination of anal, renal, limb, and ear anomalies. The two reported mutations are predicted to result in a prematurely terminated HSAL-1 lacking all double zinc finger domains, and to cause TBS in heterozygous patients. Other vertebrate *sal* genes may also be finely

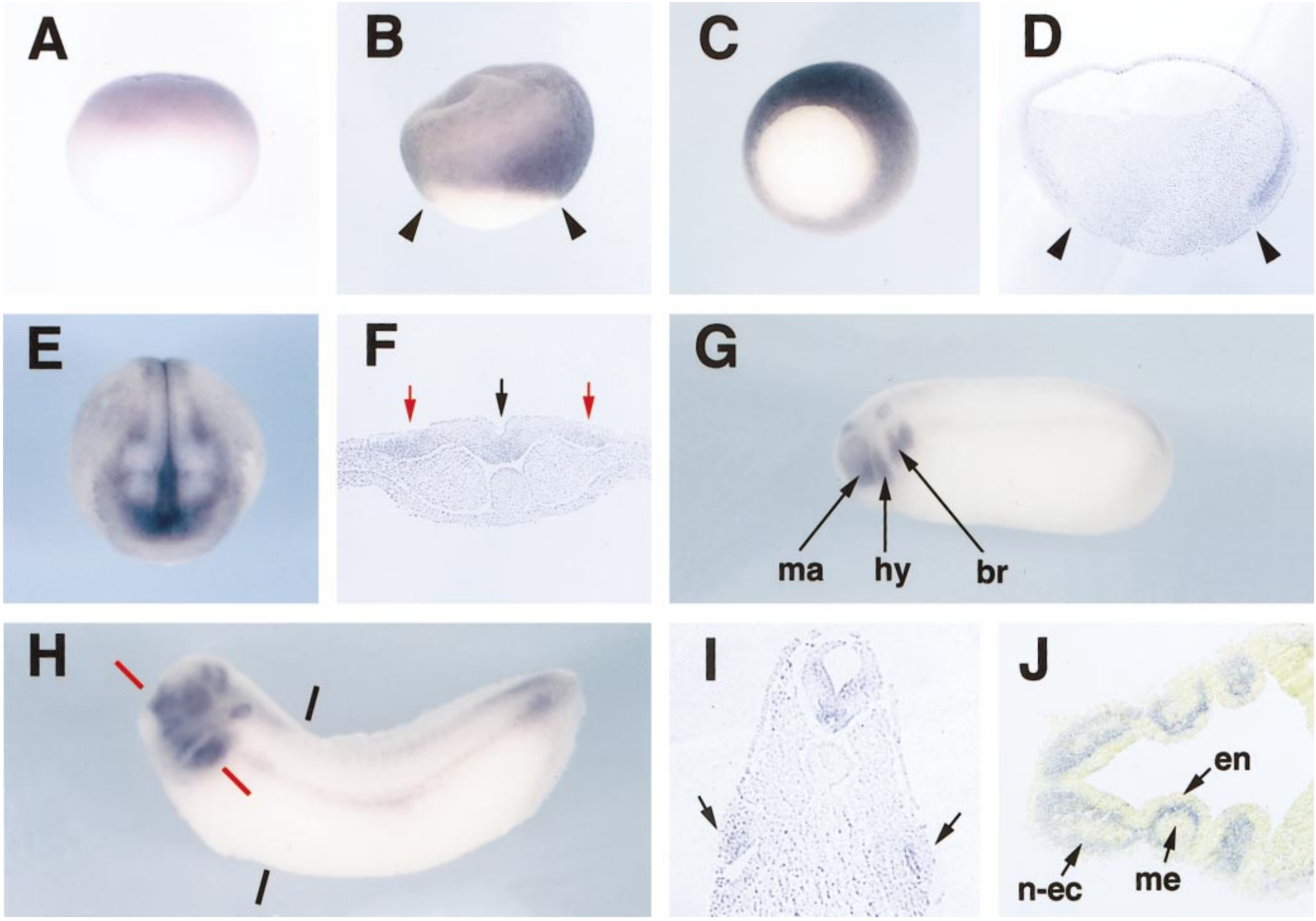

FIG. 4. Pattern of expression of *Xsal-3* during development shown by whole-mount *in situ* hybridization and sections of stained embryos. (A) Lateral view of an unfertilized egg. The animal pole is at the top. (B) Lateral view of a stage 11 embryo. The blastopore site is indicated by the arrowhead. (C) Vegetal view of a stage 11 embryo. The dorsal side is at the top. (D) A sagittal section of the stage 11 embryo in B. The blastopore site is indicated by the arrowhead. (E) Anterior view of a stage 16 embryo. (F) Transverse section of the stage 16 embryo in E. *Xsal-3* is expressed in the neural plate (black arrow) along the anteroposterior axis and the neural crest (red arrows). (G) Lateral view of a stage 25 embryo. *Xsal-3* expression appears in the pronephric duct. And the mandibular (ma), hyoid (hy) and branchial (br) (anterior plus posterior) arches are clearly seen. (H) Lateral view of a stage 30 embryo. The black and red lines indicate the plane of the section shown in I and J. (I) Transverse section of the stage 30 embryo in H. Expressions is seen in the neural tube and the pronephric duct (arrow). (J) Horizontal section of the stage 30 embryo. *Xsal-3* is expressed only in the neuroectoderm. n-ec, neuroectoderm; en, endoderm; me, mesoderm.

regulated and have important roles during development. We examined overexpression of long or short form *Xsal-3* in *Xenopus* early embryos, but no phenotypic changes were observed (data not shown). The deficiency of SAL protein dosage may be more crucial in embryogenesis. Further studies are required to disclose which factors regulate *Xsal-3,* and are regulated by *Xsal-3,* during *Xenopus* embryogenesis.

ACKNOWLEDGMENTS

This work was supported in part by grants from the Ministry of Education, Science, Sports, and Culture, Japan; and by CREST (Core Research for Evolution Science and Technology) of the Japan Science and Technology Corporation. We thank Dr. Yuzuru Eto of the Central Research Laboratories of Ajinomoto Co. Inc. for providing human recombinant activin A. Department of Stem Cell Regulation is supported by AMGEN Limited.

REFERENCES

1. Jürgens, G. (1988) *EMBO J.* **7,** 189–196.
2. Kühnlen, R. P., Frommer, G., Friedrich, M., Gonzalez-Gaitan, M., Weber, A., Wagner-Bernholz, J. F., Gehring, W. J., Jäckle, H., and Schuh, R. (1994) *EMBO J.* **13,** 168–179.
3. Kaptein, R. (1991) *Curr. Opin. Struct. Biol.* **2,** 109–115.
4. Berg, J. M. (1990) *Annu. Rev. Biophys. Biophys. Chem.* **19,** 405–421.
5. Kohlhase, J., Wischermann, A., Reichenbach, H., Foster, U., and Engel, W. (1998) *Nat. Genet.* **18,** 81–83.
6. Köster, R., Stick, R., Loosli, F., and Wittbrodt, J. (1997) *Development* **124,** 3147–3156.

7. Hollemann, T., Schuh, R., Pieler, T., and Stick, R. (1996) *Mech. Dev.* **55,** 19–32.
8. Nieuwkoop, P. D., and Faber, J. (1967) Normal Table of *Xenopus laevis* (Daudin). North-Holland, Amsterdam.
9. Hemmati-Brivanlou, A., de la Torr, J. R., Holt, C., and Harland, R. M. (1991) *Development* **111,** 715–724.
10. Bassez, T., Paris, J., Omilli, F., Dorel, C., and Osborne, H. B. (1990) *Development* **110,** 955–962.
11. Osborne, H. B., Dorel, C., Ghoba, L., Omilli, F., Bassez, T., and Coffino, P. (1991) *Eur. J. Biochem.* **202,** 575–581.
12. Harland, R. M. (1991) *in* Methods in Cell Biology (Kay, B. K., and Peng, H. J., Eds.), Vol. 36, pp. 685–695. Academic Press, San Diego.
13. Uochi, T., and Asashima, M. (1996) *Dev. Growth Differ.* **38,** 625–634.
14. Kohlhase, J., Schuh, R., Dowe, G., Kühnlen, R. P., Jäckle, H., Schroeder, B., Schulz-Schaeffer, W., Kretzschmar, H. A., Köhler, A., Müller, U., Raab-Vetter, M., Burkhardt, E., Engel, W., and Stick, R. (1996) *Genomics* **38,** 291–298.
15. Ott, T., Kaestner, K. H., Monaghan, A. P., and Schütz, G. (1996) *Mech. Dev.* **56,** 117–128.
16. de Celis, J. F., Barrio, R., and Kafatos, F. C. (1996) *Nature* **381,** 421–424.
17. Nellen, D., Burke, R., Struhl, G., and Basler, K. (1996) *Cell* **85,** 357–368.
18. Chiang, C., Litingtung, Y., Lee, E., Young, K. E., Corden, J. L., Westphal, H., and Beachy, P. A. (1996) *Nature* **383,** 407–413.
19. Roberts, D. J., Johnson R. L., Burke A. C., Nelson C. E., Morgan B. A., and Tabin C. (1995) *Development* **121,** 3163–3174.